RSC Advances c3ra44659j

COMMUNICATION

1

A novel aluminium–air secondary battery with long-term stability

Ryohei Mori*

An aluminium–air secondary battery was fabricated by using an aluminium ion conductor, $Al_2(WO_4)_3$, and plain salt water as an electrolyte.

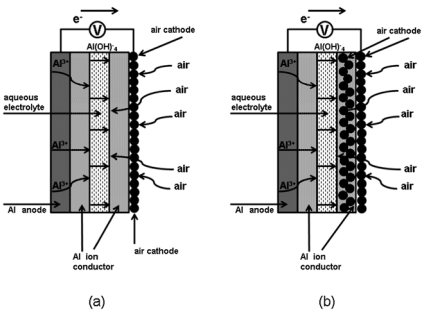

Please check this proof carefully. **Our staff will not read it in detail after you have returned it.**

Translation errors between word-processor files and typesetting systems can occur so the whole proof needs to be read. Please pay particular attention to: tabulated material; equations; numerical data; figures and graphics; and references. If you have not already indicated the corresponding author(s) please mark their name(s) with an asterisk. Please e-mail a list of corrections or the PDF with electronic notes attached - do not change the text within the PDF file or send a revised manuscript. Corrections at this stage should be minor and not involve extensive changes. All corrections must be sent at the same time.

Please bear in mind that minor layout improvements, e.g. in line breaking, table widths and graphic placement, are routinely applied to the final version.

We will publish articles on the web as soon as possible after receiving your corrections; **no late corrections will be made.**

Please return your **final** corrections, where possible within **48 hours** of receipt by e-mail to: advances@rsc.org

Queries for the attention of the authors

Journal: RSC Advances

Paper: c3ra44659j

Title: A novel aluminium--air secondary battery with long-term stability

Editor's queries are marked like this... 1, and for your convenience line numbers are inserted like this... 5

Please ensure that all queries are answered when returning your proof corrections so that publication of your article is not delayed.

Query Reference	Query	Remarks
1	For your information: You can cite this article before you receive notification of the page numbers by using the following format: (authors), RSC Adv., (year), DOI: 10.1039/c3ra44659j.	
2	Please carefully check the spelling of all author names. This is important for the correct indexing and future citation of your article. No late corrections can be made.	
3	Please check that the inserted GA image and text are suitable.	
4	Please indicate where ref. 16 should be cited in the text.	

RSC Advances

COMMUNICATION

A novel aluminium–air secondary battery with long-term stability

Ryohei Mori*

Cite this: DOI: 10.1039/c3ra44659j

Received 25th August 2013
Accepted 15th November 2013

DOI: 10.1039/c3ra44659j

www.rsc.org/advances

An aluminium–air secondary battery was fabricated by using an aluminium ion conductor, $Al_2(WO_4)_3$, and plain salt water as an electrolyte. The battery functioned for approximately one month. It was also possible to enhance the cell capacity and suppress the yield of by-products, by modifying the cell structure.

There is an urgent need for clean fuel alternatives for energy supply and storage created by fossil fuel depletion and air pollution arising from combustion.[1,2] To this end, metal–air batteries have garnered attention as potential high-performance power sources for electronic devices,[3,4] of which lithium–air cells are the most promising for high-performance applications.[5,6] However, lithium is sensitive to ambient conditions such as humidity and oxygen, and is a scarce natural resource in some regions.

Aluminium, in contrast, is an abundant, attractive anode material for energy storage and conversion because of its high specific capacity, highly negative standard electrode potential [$E^\circ = -1.7$ V *vs.* standard hydrogen electrode (SHE)], and environmentally benign characteristics. In addition, aluminium is the most recycled metal in the world and is relatively inexpensive. When compared with zinc, lithium, and other metals, aluminium has unique advantages and disadvantages. Its relatively low atomic weight of 26.98 and trivalence confer it a gram-equivalent weight of 8.99 and an electrochemical equivalence of 2.98 A h^{-1} g^{-1}, compared with 3.86 A h^{-1} g^{-1} for lithium, 2.20 A h^{-1} g^{-1} for magnesium, and 0.82 A h^{-1} g^{-1} for zinc. Moreover, on a per-volume basis, aluminium yields 8.04 A h^{-1} cm^{-3}, compared with 2.06 A h^{-1} cm^{-3} for lithium, 3.83 A h^{-1} cm^{-3} for magnesium, and 5.85 A h^{-1} cm^{-3} for zinc.[7]

A major barrier to commercialization is aluminium's high self-corrosion rate in alkaline solutions, both under open-circuit conditions and during discharge. To reduce the self-corrosion of the aluminium anode, two methods are usually employed: alloying aluminium with other elements[8–10] or modifying the composition of the electrolyte.[11–15] However, these research has been largely unsuccessful for the commercial production of Al–air cells because by-products such as Al_2O_3 and $Al(OH)_3$ accumulate at both the anode and cathode. Therefore, we propose to cover the aluminium anode and the air cathode with ceramic aluminium ion conductors, preventing anode corrosion resulting from direct contact with the electrolyte, while retaining aluminium ion conduction. In addition, this method may prevent by-product accumulation and suppress electrolyte evaporation (the major drawback of all metal–air batteries).

In a previous study of ours, $Al_2(WO_4)_3$ was used as an aluminium ion conductor on both the anode and air cathode, and we succeeded in preparing an Al–air cell with secondary battery properties that was stable for one week.[17] However, by-products such as Al_2O_3 and $Al(OH)_3$ still formed on the aluminium ion conductor at both the anode and the cathode.

In this study, by using a plain salt water as an electrolyte, we have fabricated an Al–air cell which functioned for approximately 1 month with the absence of Al_2O_3 and $Al(OH)_3$. Furthermore, the cell capacity was largely enhanced by combining conductive carbon and ceramic aluminium ion conductor as the air cathode material.

In our previous study, the Al–air cell was termed AFLA as an acronym of its major components: an aluminium anode, an $Al_2(WO_4)_3$ film, an $Al_2(WO_4)_3$ lid, and an air cathode[17] (Fig. 1). (We refer to the material which covers the air cathode as the "lid".) An aluminium board was used as the anode. The air cathode was composed of conductive carbon and polyvinylidenedifluoride (PVDF) dissolved in *N*-methyl-pyrrolidone on a nickel mesh current collector. The $Al_2(WO_4)_3$ film was prepared by coating the aluminium anode with a printing slurry composed of $Al_2(WO_4)_3$ powder and terpineol, followed by annealing at 500 °C. A 10% NaCl aqueous solution was used as the electrolyte. The pH of the electrolyte was adjusted to 6.7–6.8.

In this study we prepared Al–air cells with two different lid compositions. The first lid was made of $Al_2(WO_4)_3$ (AFLA-A cell); the second lid was a mixture of $Al_2(WO_4)_3$ and conductive carbon

Fuji Pigment Co.Ltd, 2-23-2 Obana, Kawanishi-city, Hyogo Prefecture 666-0015, Japan. E-mail: moriryohei@fuji-pigment.co.jp; Fax: +81-72-7599008; Tel: +81-72-7598501

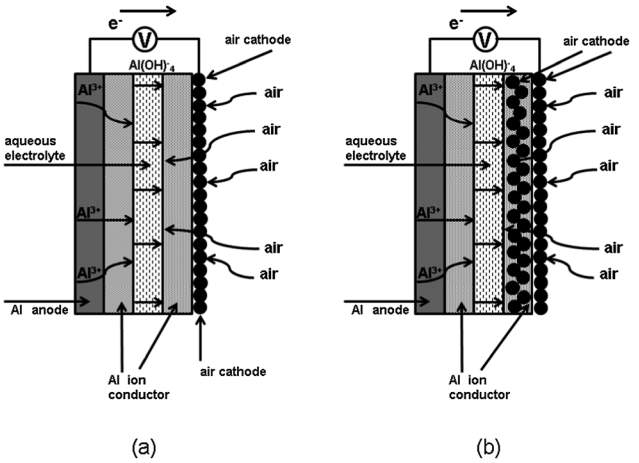

Fig. 1 A schematic figure of AFLA cell: (a) AFLA-A cell and (b) AFLA-AC cell.

(AFLA-AC cell). The powders were mixed in respective ratios of 9 : 0 : 1 and 8 : 1 : 1 ($Al_2(WO_4)_3$: carbon : PVDF), and pressed into disks. The structure of the prepared cells can be summarized as Al | $Al_2(WO_4)_3$|NaCl | $Al_2(WO_4)_3$| air cathode (AFLA-A, Fig. 1(a)) and Al | $Al_2(WO_4)_3$|NaCl | $Al_2(WO_4)_3$ + carbon | air cathode (AFLA-AC, Fig. 1(b)).

Fig. 2 show fifteen discharge curves of the prepared Al–air cells at an applied current of 0.2 μA (cm^{-2}) for the AFLA-A cell and 0.1 mA (cm^{-2}) for the AFLA-AC cell. The cut-off potential was 0.2 V. for AFLC-A cell, the capacity was initially 8.96 μA h cm^{-2}, but dropped to 8.85 μA h cm^{-2} and 8.29 μA h cm^{-2} at the 5th and 15th cycles, respectively. Capacity is smaller than previous study when NaOH was used as an electrolyte (Fig. 3).[17]

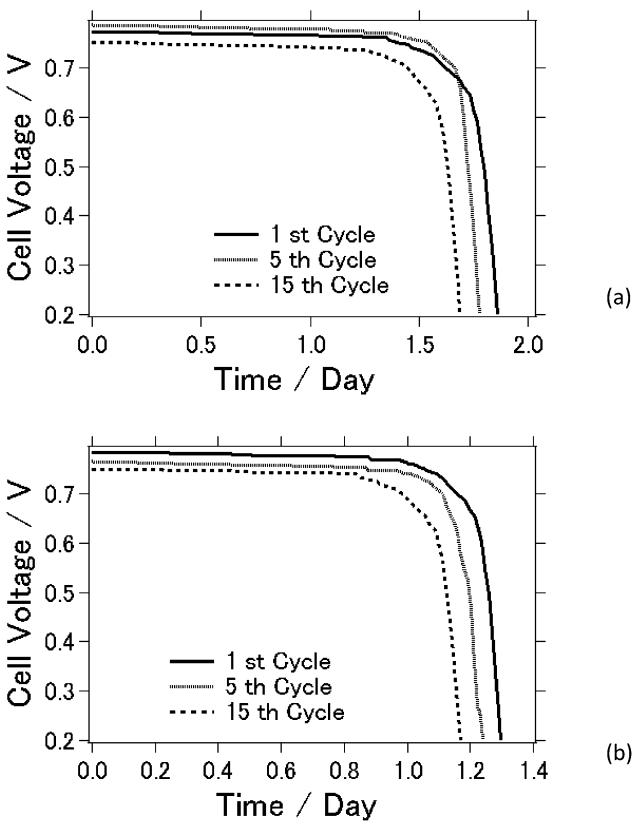

Fig. 2 Discharge curve of Al–air cells: (a) AFLA-A cell and (b) AFLA-AC cell.

Generally, cell capacity is larger when NaOH was used as an electrolyte.[7] However. at the AFLA-AC cell, even with NaCl electrolyte, the initial capacity was 3.12 mA h cm^{-2}, but dropped to 3.04 mA h cm^{-2} and 2.95 mA h cm^{-2} at the 5th and 15th cycles, respectively. This large capacity difference is responsible for the applied current differing between the AFLA-A and AFLA-AC cells. It is obvious that the cell capacity is much larger in the AFLA-AC cell.

However, we had observed that capacity and voltage faded with cycle number. We suggest this fading is due to deterioration of the AFLA cell itself. The AFLA cell is under development as a secondary battery and not yet robust enough. We especially suggest that the "lid" needs to be strengthened in order to maintain high capacity and voltage even after long-term use.

At the air cathode, the water in the electrolyte reacts with oxygen from the air:

$$O_2 + 2H_2O + 4e^- \rightarrow 4OH^-$$

This reaction is accelerated by the close proximity of the electrolyte to the conductive carbon, which is an active air cathode material. In other words, existence of conductive carbon as electron conductor in the lid, electron migration was accelerated in the AFLA-AC cell. We propose that this is the main reason for the enhanced capacity. However, as the reviewer points out that this is only a suggestion. In order to investigate this issue, we will need to conduct more-detailed future research. For example, we could see the effect of varying carbon content in the lid. Furthermore, we could attempt to use other types of air cathode materials such as active carbon, Mn_2O_3 and $LaFeO_3$ to investigate variation in conductivity and performance even further.[18–20] In addition, both the AFLA-A and ALFA-AC cells exhibited stable discharge capacity for fifteen

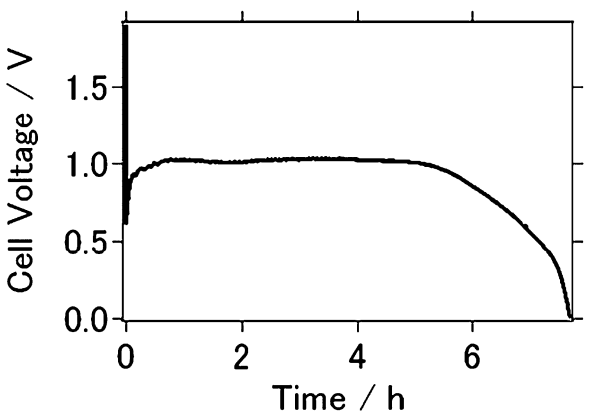

Fig. 3 Discharge curve of Al–air cell from previous article ref. 17.

cycles, suggesting that they were quite stable when NaCl was used as the electrolyte.

Fig. 4(a)–(d) display charge–discharge curves collected over twenty-eight days at an applied current of 0.2 μA (cm^{-2}) for the AFLA-A cell and 0.1 mA (cm^{-2}) for the AFLA-AC cell. Each figure displays the charge–discharge curves of the first and last four days of the measurement period. To the best of our knowledge, this is the longest measurement period reported for charge–discharge curves of an Al–air cell.[21,22] Previous studies regarding Li–Air battery performance similarly provided data of charge–discharge voltage against time to evaluate secondary battery functionality.[23–25] However, it should be noted here that due to evaporation of the electrolyte, the NaCl solution was refilled once every five days to ensure sufficient electrical contact. We suggest that the electrolyte evaporation was attributable to macro- and micropores formed in the lid because of the simplicity of the lid preparation technique. This issue needs to be further investigated and improved for future study.[26]

Fig. 5 shows the voltage profiles of the AFLA-AC cell as a function of the time. The cell was discharged galvanostatically under different rates from 0.05 mA cm^{-2} to 0.5 mA cm^{-2}. The cut-off voltage was 0.1 V in all cases. At discharge rates

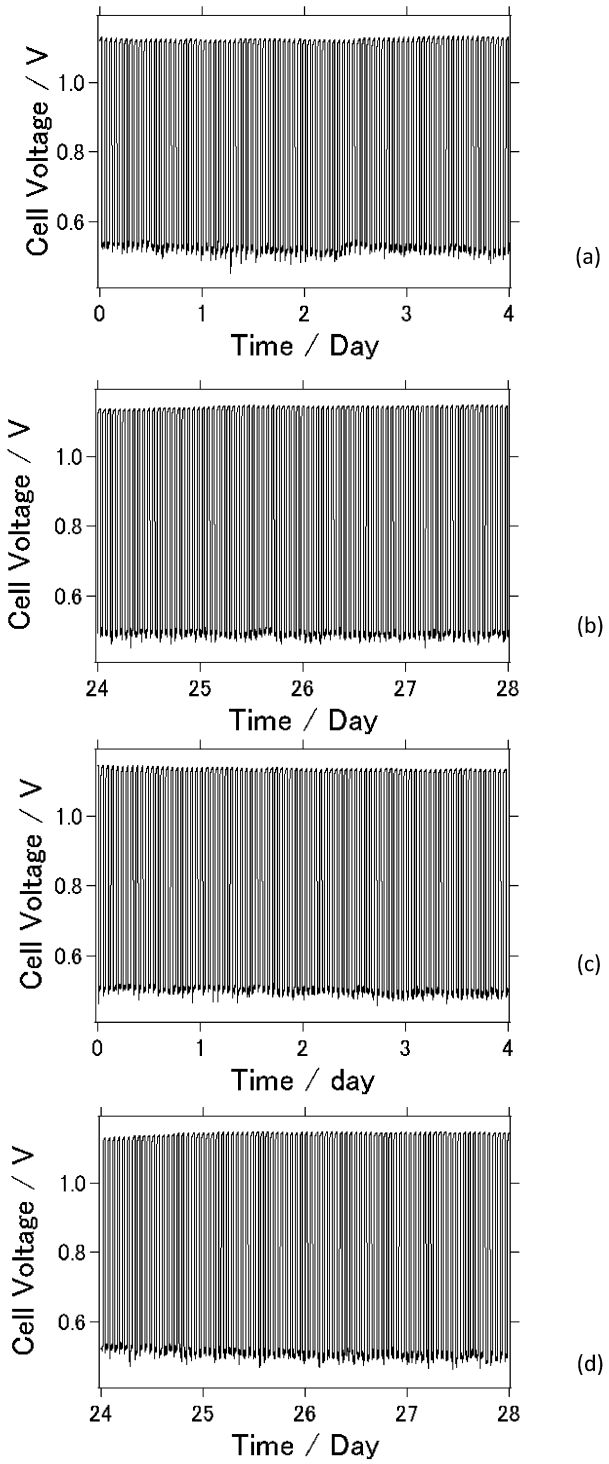

Fig. 4 Charge–discharge curve of AFLA cell. (a) 1st four days of AFLA-A cell. (b) Last four days of AFLA-A cell. (c) 1st four days of AFLA-AC cell. (d) Last four days of AFLA-AC cell.

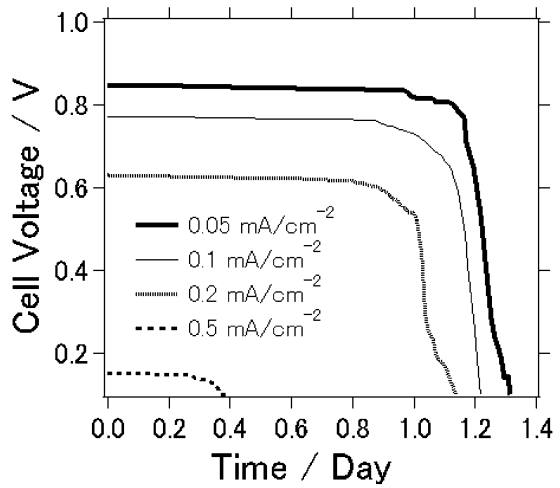

Fig. 5 Discharge curves of AFLA-AC cell at different discharge rates.

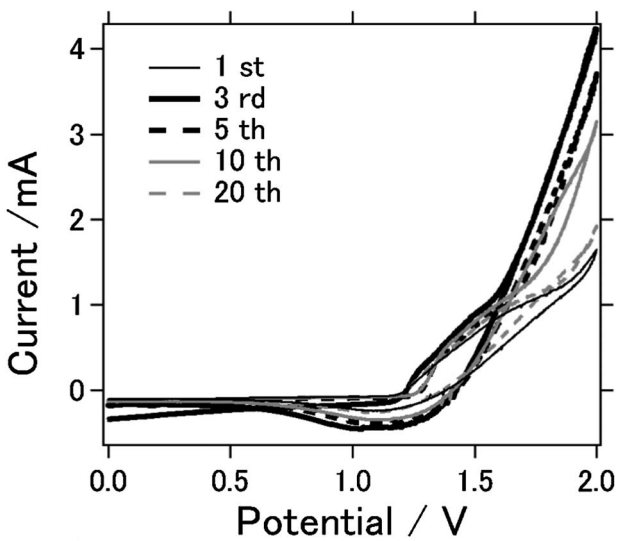

Fig. 6 Cyclic votammograms of AFLA-AC cell.

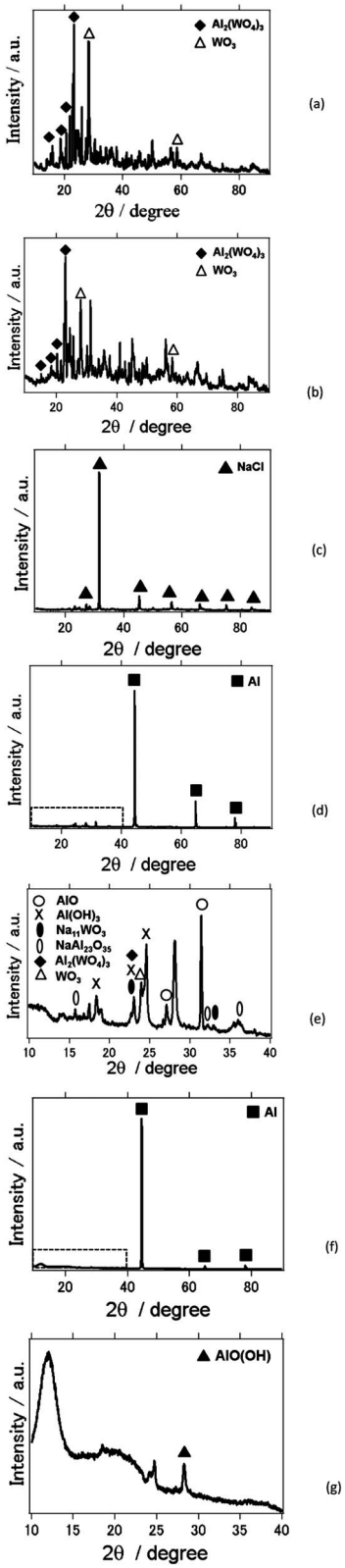

Fig. 7 X-ray diffraction pattern of materials prepared in this study: (a) $Al_2(WO_4)_3$ powder purchased for this study, (b) the lid after charge–discharge reaction for one month with NaCl electrolyte for AFLA-A Cell. (c) The lid after charge-discharge reaction for one month with NaCl electrolyte for AFLA-AC Cell. (d) The film after charge-discharge reaction for one month with NaCl electrolyte for AFLA-A Cell. (e) Magnified image of Fig. 4(d) between 10 and 40 degrees in 2θ. (f) The film after charge-discharge reaction for one month with NaCl electrolyte for AFLA-AC Cell. (g) Magnified image of Fig. 4(f) between 10 and 40 degrees in 2θ.

between 0.05 and 0.2 mA cm^{-2}, the voltage profiles were kept almost constant. With increasing discharge rates, the progressive decline of discharge voltage was observed. When discharge current was 0.05 mA cm^{-2}, the capacity was 1.572 mA h cm^{-2}. As discharge current increases as 0.1,and 0.2 mA h cm^{-2}, the capacity were 2.904 and 5.472 mA h cm^{-2}, respectively. But for 0.5 mA cm^{-2}, the discharge curve of cell became a slope instead of plateau, and discharge capacity decreased to 4.68 mA h cm^{-2}.

Fig. 6 is the cyclic voltammograms of the AFLA-AC cell for the first, 3rd, 5th, 10th and 20th cycles measured between 0 and 2.0 V to characterize the redox reactions. Anodic current increases largely at the 3rd cycle compared to 1st cycle, although anodic current lowers as cycle number increases and become similar to the 1st current (at 20 th cycle). The reduction and oxidation peak positions for every cycle's are relatively the same at 1.2–1.3 V and 1.4–1.5 V respectively. This demonstrates that the redox pairs contribute to the gain and loss of electrons in AFLA-AC cell during cell charge–discharge reaction. The reason for high intensities at 3–10 th cycle is unknown, however this fact indicates the higher electrochemical reactivity at 3–10 th cycle.

Fig. 7 shows X-ray diffraction patterns of the $Al_2(WO_4)_3$ powder, lid, and film, before and after each experiment. Fig. 7(a) shows the X-ray diffraction pattern of the commercially available $Al_2(WO_4)_3$ powder used in this study, which was composed of $Al_2(WO_4)_3$ and WO_3 phases. After one month of charge–discharge experiments, the lid composed of $Al_2(WO_4)_3$ still exhibited both $Al_2(WO_4)_3$ and WO_3 phases (Fig. 7(b)). On the other hand, the lid composed of $Al_2(WO_4)_3$ and carbon had a NaCl phase after the same period (Fig. 7(c)). Fig. 7(d) shows the X-ray analysis result of the $Al_2(WO_4)_3$ film of the AFLA-A. The $Al_2(WO_4)_3$ film had dissolved and an Al metal phase originating from the substrate was detected. Fig. 7(e) displays the magnified image of Fig. 7(d) between 10 and 40 degrees in 2θ. $NaAl_{23}O_{35}$(β-alumina), $Na_{11}WO_3$, AlO (aluminium oxide (II)) and $Al(OH)_3$ phases were observed, and $Al_2(WO_4)_3$ was still detectable. When the lid was composed of $Al_2(WO_4)_3$ and carbon, the Al anode substrate also was exposed due to $Al_2(WO_4)_3$ dissolution and AlO(OH) (aluminium hydroxide oxide) was observed on the substrate film (Fig. 7(f) and (g)). However, typical by-products such as $AlOH_3$ and Al_2O_3 that inhibit the secondary battery reaction were not observed. One might infer that this is why we were able to run charge–discharge measurements for one month with a higher cell capacity than for the AFLA-A cell.

We attempt to explain the yield of the different crystalline phases on the anode as compared to when a NaOH electrolyte was used in our previous study, by analyzing the reactions taking place using a NaCl electrolyte.[27]

OH^- is produced at the cathode as in the following reaction:

$$O_2 + 2H_2O + 4e^- \rightarrow 4OH^-$$

Then, OH^- migrates through the electrolyte to reach the Al anode, where the following discharge reaction occurs:[22]

$$Al + 4OH^- \rightarrow Al(OH)_4^- + 3e^-$$

However, OH^- must first transit the $Al_2(WO_4)_3$ thin film before reaching the Al metal anode. We reason that the porosity of the Al ion conductor due to our nano-size particle dispersion preparation method is responsible for allowing OH^- to travel through pores in the Al ion conductor film and reach the Al anode in order to continue the reaction.

Hence, the overall Al–air cell reaction is:

$$4Al + 3O_2 + 6H_2O + 4OH^- \rightarrow 4Al(OH)_4^-$$

Eventually, aluminium hydroxide precipitates:

$$Al(OH)_4^- \rightarrow Al(OH)_3 + OH^-$$

In our previous study, when NaOH was used as the electrolyte, $AlOH_3$ and Al_2O_3 were observed in the film and the lid. When NaOH was used as an electrolyte, $Al(OH)_3^-$ is the charge-carrying ion species.[28] On the other hand, when NaCl is used as an electrolyte, $Al(OH)_3^-$ and transitory compounds such as $Al(OH)_2Cl$, $Al(OH)Cl_2$, and $AlCl_3$ are the charge carriers.[29] These different charge-carrying species may be the reason for the yields of different crystalline phases at the anode. Thus far, the typical by-products of the aluminium ion battery that inhibit the cell reaction have been reported to be $Al(OH)_3$ and Al_2O_3.[30] In this study, various types of other chemicals were detected, including $NaAl_{23}O_{35}$, $Na_{11}WO_3$, AlO and AlO(OH). For example, β-alumina is known to be a good sodium ion conductor and has been used as a solid electrolyte in NaS batteries.[31] However, the influence of these chemicals needs to be clarified since their effects on aluminium air batteries have not yet been studied.[7] On the other hand, a different crystalline phase precipitated on the lid after the measurement. In fact, when the lid was soaked in aqueous NaCl without applying an electrical bias, the X-ray diffraction showed evidence of phases of $Al_2(WO_3)_4$ in the AFLA-A cell and NaCl in the AFLA-AC cell, respectively (data not shown). One can infer that NaCl tends to precipitate on carbon more readily than on $Al_2(WO_3)_4$.

Conclusions

We successfully assembled a functional Al–air cell with an AFLA structure using plain salt water as an electrolyte. Moreover, by combining the air cathode active material and the solid electrolyte, we were able to achieve a higher cell capacity. Future work will be required to fabricate a cell in which the aluminium ion conductor film does not dissolve at the anode, by using either another electrolyte or another aluminium ion conductor with better Al^{3+} conductivity.[32,33] Importantly, we have shown that aluminium is a reasonable option for a secondary cell material, as it is more abundant, safer, and easier to handle than other candidate metals such as lithium, zinc, magnesium, and sodium.

Acknowledgements

The author wishes to express thanks to Dr Sadayoshi. Mori and Mr.Kazuo Sakai for helpful discussions.

Notes and references

1 R. Padbury and X. Zhang, *J. Power Sources*, 2011, **196**, 4436–4444.
2 J. Chen, J. S. Hummelshøj, K. S. Thygesen, J. S. G. Myrdal, J. K. Nørskov and T. Vegge, *Catal. Today*, 2011, **165**, 2–9.
3 P. Kichambare, J. Kumar, S. Rodrigues and B. Kumar, *J. Power Sources*, 2011, **196**, 3310–3316.
4 M. Armand and J. Tarascon, *Nature*, 2008, **451**, 652–657.
5 G. Girishkumar, B. McCloskey, A. Luntz, S. Swanson and W. Wilcke, *J. Phys. Chem. Lett.*, 2010, **1**, 2193–2203.
6 F. Wagner, B. Lakshmanan and M. Mathias, *J. Phys. Chem. Lett.*, 2010, **1**, 2204–2219.
7 Q. Li and N. Bjerrum, *J. Power Sources*, 2002, **110**, 1–10.
8 S. Abedin and A. Saleh, *J. Appl. Electrochem.*, 2004, **34**, 331–335.
9 M. Krishnan and N. Subramanyan, *Corros. Sci.*, 1977, **17**, 893–900.
10 M. Paramasivam and S. Iyer, *J. Appl. Electrochem.*, 2001, **31**, 115–119.
11 D. Macdonald and C. English, *J. Appl. Electrochem.*, 1990, **20**, 405–417.
12 H. Shao, J. Wang, Z. Zhang, J. Zhang and C. Cao, *Mater. Chem. Phys.*, 2002, **77**, 305–309.
13 Y. Ein-Eli, M. Auinat and D. Starrosvetsky, *J. Power Sources*, 2003, **114**, 330–337.
14 A. Maayta and N. Al-Rawashdeh, *Corros. Sci.*, 2004, **46**, 1129–1140.
15 A. Mukherjee and I. Basumallick, *J. Power Sources*, 1996, **58**, 183–187.
16 S. Licht, R. Tel-Vered, G. Levitin and C. Yarnitzky, *J. Electrochem. Soc.*, 2000, **2**, 496–501.
17 R. Mori, *RSC Adv.*, 2013, **3**, 11547–11551.
18 H. Dong, H. Yu and X. Wang, *Environ. Sci. Technol.*, 2012, **46**, 13009–13015.
19 M. Augustin, O. Yezerska, H. Borchert, T. Plaggenborg and D. Fenske, *ECS Trans.*, 2013, **45**, 1–10.
20 T. Takeguchi, *et al.*, *J. Am. Chem. Soc.*, 2013, **135**, 11125–11130.
21 J. B. Wang, J. M. Wang, H. B. Shao, X. T. Chang, L. Wang, J. Q. Zhang and C. N. Cao, *Mater. Corros.*, 2009, **60**, 269–273.
22 M. Nestoridi, D. Pletcher, R. J. K. Wood, S. Wang, R. L. Jones, K. R. Stokes and I. Wilcock, *J. Power Sources*, 2008, **178**, 445–455.
23 E. Yoo and H. Zhou, *J. Power Sources*, 2013, **244**, 429–434.
24 Y. Wang, P. He and H. Zhou, *Adv. Energy Mater.*, 2012, **2**, 770–779.
25 E. Yoo and H. Zhou, *ACS Nano*, 2011, **5**, 3020–3026.

26 R. Mori, T. Ueta, K. Sakai, Y. Niida, Y. Koshiba, L. Lei, K. Yamaguchi, K. Nakamae and Y. Ueda, *J. Mater. Sci.*, 2011, **46**, 1341–1350.
27 A. A. Mohamad, *Corros. Sci.*, 2008, **50**, 3475–3479.
28 S. I. Pyun and S. Y. Moon, *J. Solid State Electrochem.*, 2000, **4**, 267–272.
29 K. Y. Chan and R. F. Savinell, *J. Electrochem. Soc.*, 1991, **138**, 1976–1984.
30 A. M. Abdel-Gaber, E. Khamis, H. Abo-ELDahab and S. Adeel, *Mater. Chem. Phys.*, 2008, **109**, 297–305.
31 Z. Wen, J. Cao, Z. Gu, X. Xu, F. Zhang and Z. Lin, *Solid State Ionics*, 2008, **179**, 1697–1701.
32 N. Imanaka and S. Tamura, *Bull. Chem. Soc. Jpn.*, 2011, **84**, 353–362.
33 N. Imanaka, Y. Hasegawa, M. Yamaguchi, M. Itaya, S. Tamura and G. Adachi, *Chem. Mater.*, 2002, **14**, 4481–4483.